IEEE Access
Multidisciplinary | Rapid Review | Open Access Journal

Received August 9, 2021, accepted August 16, 2021, date of publication August 27, 2021, date of current version October 15, 2021.

Digital Object Identifier 10.1109/ACCESS.2021.3108453

Spatial-Temporal Genetic-Based Attention Networks for Short-Term Photovoltaic Power Forecasting

TAO FAN[1], TAO SUN[2], HU LIU[1], XIANGYING XIE[2], AND ZHIXIONG NA[2]
[1]State Grid Corporation of China, Beijing 100031, China
[2]State Grid E-Commerce Company Ltd., Beijing 100053, China

Corresponding author: Zhixiong Na (hellonazx@163.com)

This work was supported in part by the National Key Research and Development Program of China under Grant 2018YFB1500800, in part by the Science and Technology Project of State Grid Corporation of China under Grant SGTJDK00DYJS2000148, and in part by the Self-Built Project of State Grid E-Commerce Company Ltd., in 2020, under Grant 1700/2020-72001B.

ABSTRACT Photovoltaic (PV) output power is significantly random and fluctuating due to its sensitivity to meteorological factors, making PV power forecasting a big challenge. Accurate short-term PV power forecasting plays a crucial role for the stable operation and maintenance management of PV systems. To achieve this target, the paper proposes a novel Spatial-Temporal Genetic-based Attention Networks (STGANet), which consists of a spatial-temporal module (STM) and a genetic-based attention module (GAM). STM serves to predict the missing solar irradiance to support the generation forecast, and contains a graph convolutional neural network to learn the spatial and temporal dependencies between historical meteorological data, while using dilated convolution as the non-linear part to simplify the network structure. The GAM efficiently explores for potential relationships in input features with attentional mechanism and uses genetic-based operation and LSTM which takes forecasting error as reference to find global optimal solutions and to avoid getting trapped in local optimal solutions. The model is verified through comparative experiment with several benchmark models using a real-world historical meteorological dataset and a power generation dataset of PV plants in southeastern China. The results have illustrated that the proposed model can provide better prediction performance in PV systems.

INDEX TERMS Photovoltaic output power forecasting, long short term memory model, attention mechanism, genetic algorithm.

I. INTRODUCTION

In recent years, with the shortage of traditional resources and the need for environment protection, the demand for Renewable Energy Sources (RESs) has increased dramatically [1]. Among all RESs, solar energy, as the most typical one, has attracted wide attention for its abundance and accessibility nearly everywhere. At the same time, it has a multitude of advantages over other forms of power generation, such as hydropower [2], [3]. As a result, the scale of Photovoltaic (PV) power generation has grown rapidly. The global PV market has continued to grow in recent years, with 99.8 GW of new capacity installed worldwide in 2018. China is the world's largest PV market with about 45 GW of new installed capacity and this growth is expected to continue at a similar or higher rate in the future.

However, the randomness, volatility, and intermittence of PV power generation which because of its dependence on immediate meteorological factors such as atmospheric temperature, total cloud cover, and humidity makes it more challenging to utilize than traditional generation sources [4]. In some distributed photovoltaic power plants, the precise measurement of meteorological factors is often ignored, which brings more difficulties to the prediction of power generation. These uncertainties can degrade real-time control performance, reduce system economics, and jeopardize the stable operation of the power system, thus posing significant challenges to the management and operation of the power and energy systems.

To overcome these shortcomings, accurate PV power prediction is required. Besides, it also could provide a reference

The associate editor coordinating the review of this manuscript and approving it for publication was B. Chitti Babu.

for power grid dispatching and operation of PV power stations, which is significant for security and economic efficiency [5]. PV power generation forecasts can be categorized as ultra-short-term forecast (<1 h), short-term forecast (1 h∼ 24 h), medium-term forecast (1 day ∼1 month), and long-term forecast (1 month ∼1 year). Short-term forecasting is useful for pre-scheduling and equipment maintenance to prevent improper output power. In addition, excessive or insufficient PV output power affects the safe and reliable operation of the grid, which limits the use of large grid-connected PV systems. Therefore, it is necessary to establish an accurate short-term PV prediction model to ensure the PV power stations remain stable and reliable.

Various recent researches reported different approaches to establish appropriate PV output power forecasting models aiming for higher accuracy and lower computation cost. The persistence model, as the most basic model, requires only historical data to predict PV power, and the result is equal to the actual output power of the same period of the previous day [6]. Therefore, this model usually acts as a benchmark for other models [7]. The statistical techniques generally both include the classical ones, such as the time series methods [8], regression methods [9], [10], regression trees [12], and the advanced ones, such as machine learning methods. In statistic models, the output power is forecasted by the statistical analysis of the different input variables, which include historical data and meteorological factors. The classical statistical methods play a crucial role in PV power forecasting and are easy to implement. In Semero *et al.* [10], a hybrid model with Genetic Algorithm (GA), Particle Swarm Optimization (PSO), and Adaptive Neuro-Fuzzy Inference Systems (ANFIS) was reported, which achieved superior performance of the proposed method as compared with commonly used forecasting approaches.

Machine learning methods, such as Artificial Neural Network (ANN) [14], [15], Support Vector Machine (SVM) [16], [20], Multilayer Oerceptron (MLP) [19], [21] are the most effective techniques for PV power forecasting. In dealing with non-linear data, limitations of statistical techniques due to variable meteorological factors have led to the application of artificial neural networks for predicting PV output power. Wang *et al.* [13] proposed a model using an analog plus neural network ensemble method for the very-short-term PV power forecasting and achieved great improvements. Cervone *et al.* [14] proposed a methodology based on ANN and an analog ensemble that tested on extreme-scale supercomputer simulations and outperformed each method run individually. Persson *et al.* [11] presented a non-parametric machine learning approach used for multi-site prediction of short-term PV power generation prediction, which was simple and has competitive performance. In Grimaccia *et al.* [15], a procedure to set up the main characteristics of the hybrid artificial neural networks using a physical hybrid method for day ahead PV power prediction was proposed. Malvoni *et al.* [17] developed a hybrid model with the principal component analysis and support vector machine for reducing the input data size. Jang *et al.* [18] developed a PV power forecasting model based on SVM which could have better forecasting accuracy. Paiva *et al.* [19] proved multigene genetic programming presented more accurate and robust in a single PV prediction case, whereas ANN presented more accurate results for ensemble forecasting. Huang *et al.* [21] proposed a robust genetic MLP neural network that was developed for day-ahead forecasting of hourly PV power. However, the reliability of these methods is affected by the random initial data and is sensitive to the parameters. Meanwhile, the complexity may significantly increase due to the stacked network structure.

Most currently available methods are restricted by limited data and are not able to uncover underlying correlation and related information [25]. Deep learning has been the most popular among researchers on account of its powerful capability to describe potential dependencies between data. Long Short-Term Memory network (LSTM), as one of the typical deep learning techniques, is broadly applied in PV power forecasting [26], [27]. Zhou *et al.* [27] used the stack LSTM model for adaptively focusing on input features that are more significant in forecasting, and conducted experiments with real-world photovoltaic power generation datasets. However, the output predicted by the traditional LSTM network is unstable, and methods to strengthen time linkages may fall into partial optimal solutions.

Hybrid methods [22], [24] combine two or more techniques could include advantages of both methods and exclude their limitations. Wang *et al.* [22] proposed a novel hybrid model for short-term PV output power interval forecasting based on ensemble empirical mode decomposition as well as relevance vector machine, which achieved relatively higher forecasting accuracy. Raza *et al.* [23] proposed a multivariate neural network with a Bayesian model averaging technique for predicting a day ahead PV output power. Lin *et al.* [24] proposed a multivariate neural network ensemble forecast framework, which substantially improved the forecast accuracy in short-term forecasting horizons. Chang *et al.* proposed a novel Deep Belief Network (DBN) combined with a grey theory-based data preprocessor for generation forecasting, which was superior to other models in forecasting accuracy.

In recent years, many studies based on deep learning have also been conducted. Li *et al.* [35] constructed a hybrid deep learning model combining wavelet packet decomposition (WPD) and LSTM networks for one-hour-ahead PV power forecasting. Kushwaha and Pindoriya [36] compared the accuracy of four artificial intelligence methods in forecasting Taiwan's renewable energy sources based on historical data from 2000 to 2015, and results showed that seasonal auto regressive integrated moving average random vector functional link neural network is suitable for small dataset forecast. Korkmaz *et al.* [37] used a deep CNN structure combining with Empirical Mode Decomposition (EMD) algorithm which is greatly improved the accuracy of prediction.

Yildiz and Acikgoz [38] applied an ANN-based system for very short-term (2 to 4-h) PV power forecasting. Compared with the individual LSTM-RNN networks, this model showed a superior forecasting performance.

Inspired by the previous research efforts, a novel Spatial-Temporal Genetic-based Attention Networks (STGANet) was proposed to predict day-ahead and 5 days ahead horizons. The method aims to achieve more accurate results by leveraging the interconnections of inputs and stabilizing the predicted output results. The network consists of a spatial-temporal module (STM) and a genetic-based attention module (GAM). STM consists of temporal and spatial submodules for predicting solar irradiance of PV plants without weather collectors to support power generation forecasting and contains a graph convolutional neural network to learn the spatial and temporal dependencies between historical weather data while using dilated convolution as the nonlinear part to simplify the network structure. The result combined with historical generation and weather data is used as input features for GAM. GAM combines the predicted solar irradiance and historical power generation data to predict the power generation of PV plants using an attention mechanism to efficiently explore the potential relationships in the input features and using genetic-based operations and an LSTM that takes the prediction error as a reference to find the globally optimal solution and avoid getting trapped in a locally optimal solution. The main contributions of this study are as listed:

1) We proposed a hybrid ensemble deep learning model, the spatial-temporal genetic-based attention network, considering historical meteorological and power generation data.
2) We proposed a spatial-temporal module to predict the missing solar irradiance data utilizing the spatial dependencies between photovoltaic plants.
3) We proposed a novel attention mechanism based on LSTM and genetic algorithm to predict PV power, exploring the deep connection between data and searching for the globally optimal solution.

The paper is organized as follows. Section II presents the information and analysis of real PV plants' data; Section III presents a comprehensive description of the methods applied to forecast the PV power generation; Section IV indicates the performance metrics to evaluate the forecasting models and the benchmark algorithms; Section V discusses the results of the proposed model including comparison and validations; finally, Section VI summarizes and concludes the study. The abbreviation and full name in this paper are listed in Table 1.

TABLE 1. Abbreviation and full name.

Abbreviations	Full Name
PV	Photovoltaic
STGANet	Spatial-Temporal Genetic-based Attention Networks
STM	Spatial-Temporal Module
GAM	Genetic-based Attention Module
GSO	Genetic-based Search Operator
CNN	Convolutional Neural Network
LSTM	Long Short-Term Memory
GA	Genetic Algorithm
PSO	Particle Swarm Optimization
ANFIS	Adaptive Neuro-Fuzzy Inference Systems
SVM	Support Vector Machine
MLP	Multilayer Perceptron
EMD	Empirical Mode Decomposition
WPD	Wavelet Packet Decomposition

II. DATASET ANALYSE AND PROCESSING

A. DATA DESCRIPTION AND ANALYSIS

The datasets used in the experiments are collected from three PV plants distributed in different areas in Southeastern China, 2019. Table 2 summarizes the information of the collected datasets. Output power and meteorological factors (i.e., solar irradiance, temperature, humidity, and total clouds cover) are managed separately from each power plant. The power generation data are presented at five-minute intervals, whereas the meteorological data are presented at one-hour intervals due to the limitations of the weather collection system. The meteorological data include solar irradiance, temperature, humidity and total clouds cover, where total clouds cover is expressed as percentages. Since solar irradiance can be collected only during the daytime, data from 7:00-17:00 are used in the experiment.

TABLE 2. Information of the dataset used for the experiment.

Environmental Parameters	Max	Min	Mean	Resolution	Unit
Solar irradiance	1064.71	195.68	594.51	1 hour	W/m2
Temperature	41.95	13.79	26.67	1 hour	℃
Humidity	99.23	33.00	68.15	1 hour	%RH
Total clouds cover	1.00	0.00	0.88	1 hour	%
Power	56.01	0.00	19.65	5 min	kW

Fig. 1 illustrates the daily PV output power generated by each plant for July 2019. As is shown in Fig. 1, the output power is comparatively low in the eighth and twelfth day due to the rainy or heavy cloudy weather condition. Meanwhile, output power relatively high on the days of 13, 14, and 15 in July due to the sunny weather and clear sky condition, which is because the output power fluctuates with variations in the weather conditions.

Meteorological factors strongly influence photovoltaic output power. Fig. 2(a) illustrates the pattern of PV output power for rainy or heavy cloudy days, and Fig. 2(b) illustrates the pattern of PV output power for sunny days. In abnormal weather conditions such as rainy and cloudy days, solar irradiance fluctuates without an apparent change in trend. In contrast, solar irradiance tends to increase on sunny days, peaking at noon and then decreasing. As shown in Fig. 2(a), due to the large fluctuations in solar irradiance on cloudy days, the outputs of PV power plants are also unstable. Under sunny

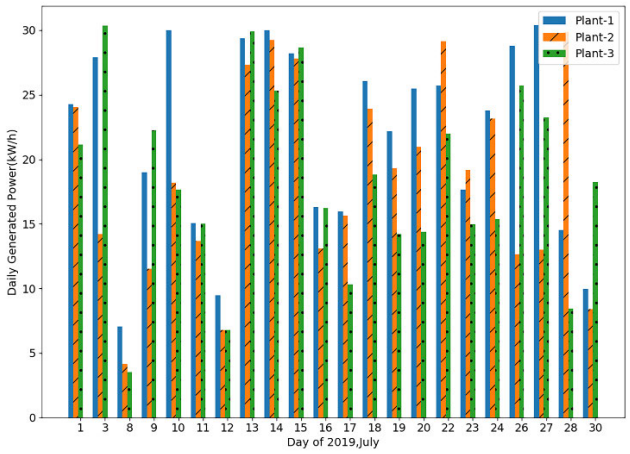

FIGURE 1. Daily output power of July 2019.

days, however, three PV plants' output tends to increase and then decrease, as does solar irradiance, indicating the PV output depends entirely on solar irradiance. Under sunny conditions, the output power of the three plants is different, and the curves fluctuate due to the various meteorological factors of the location and the influence of the PV modules on the generation of electricity.

Table 3 illustrates the correlation between the meteorological factors (i.e., solar irradiance, temperature, humidity and total clouds cover) and average PV output power.

TABLE 3. The correlation between the meteorological factors and average PV output power.

	solar irradiance	temperature	humidity	total clouds cover
Pearson correlation	0.703	0.305	-0.385	-0.38

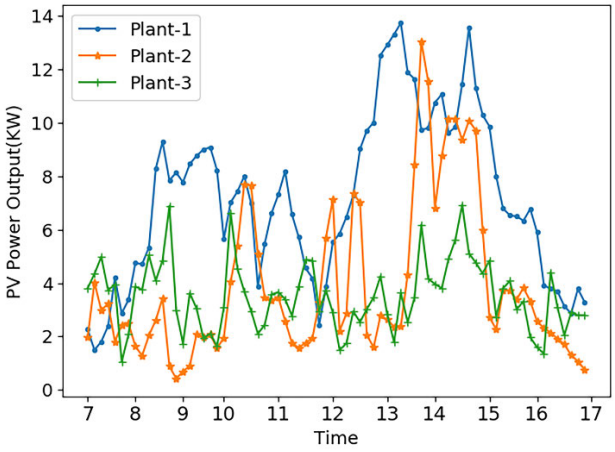

(a) Pattern of PV output power for rainy or heavy cloudy days.

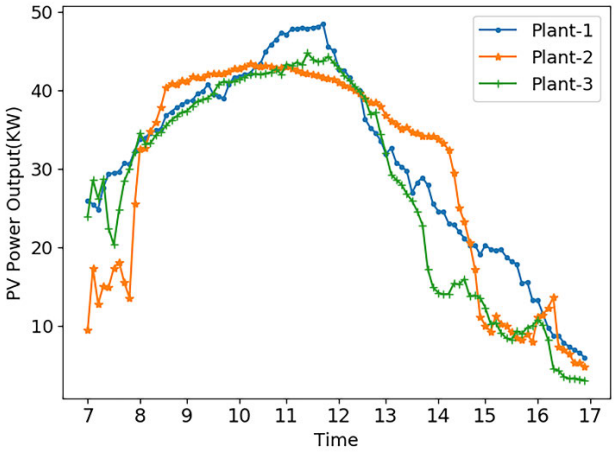

(b) Pattern of PV output power for sunny days.

FIGURE 2. Pattern of PV output power under different weather conditions.

B. DATA PRE-PROCESSING

In order to avoid large differences in data scales that can impair the effectiveness of the model, the data pre-processing is normalization, so that the data are restricted in range 0 to 1. The normalization speeds up the gradient descent to the optimal solution, increases the comparability of the data, and improves the precision of the data. The formula is:

$$x'_{in} = \frac{x_{in} - \min(x_{in})}{\max(x_{in}) - \min(x_{in})} \tag{1}$$

where x'_{in} is the normalized input data; x_{in} is the origin input data(PV output power and meteorological factors data); and max (.) and min(.) are the maximum and minimum values of the origin input data, respectively.

III. METHODOLOGY DESCRIPTION

A. OVERVIEW

In practical application, weather factors in distributed photovoltaic power stations are not precisely collected, which brings great difficulties to power generation prediction. Therefore, the whole process is divided into two parts. Firstly, the meteorological factors are predicted, and then the power generation is predicted.

The overall framework of the proposed model is illustrated in Fig. 3. Our proposed STGANet consists of a spatial-temporal module (STM) and a genetic-based attention module(GAM). The STM is used to predict the missing meteorological information, and the GAM uses the meteorological information obtained from STM and historical power generation data to forecast power generation. STM contains two temporal sub-modules, a spatial sub-module in the middle and a fully connected layer in the end. The STM processes the input data uniformly to jointly explore spatial and temporal dependencies and then generates integrated features by the output layer to generate the final meteorological prediction. The GAM firstly constructs the input matrix consisting of historical generation data and meteorology data by sliding window, secondly generates the weights of the input matrix

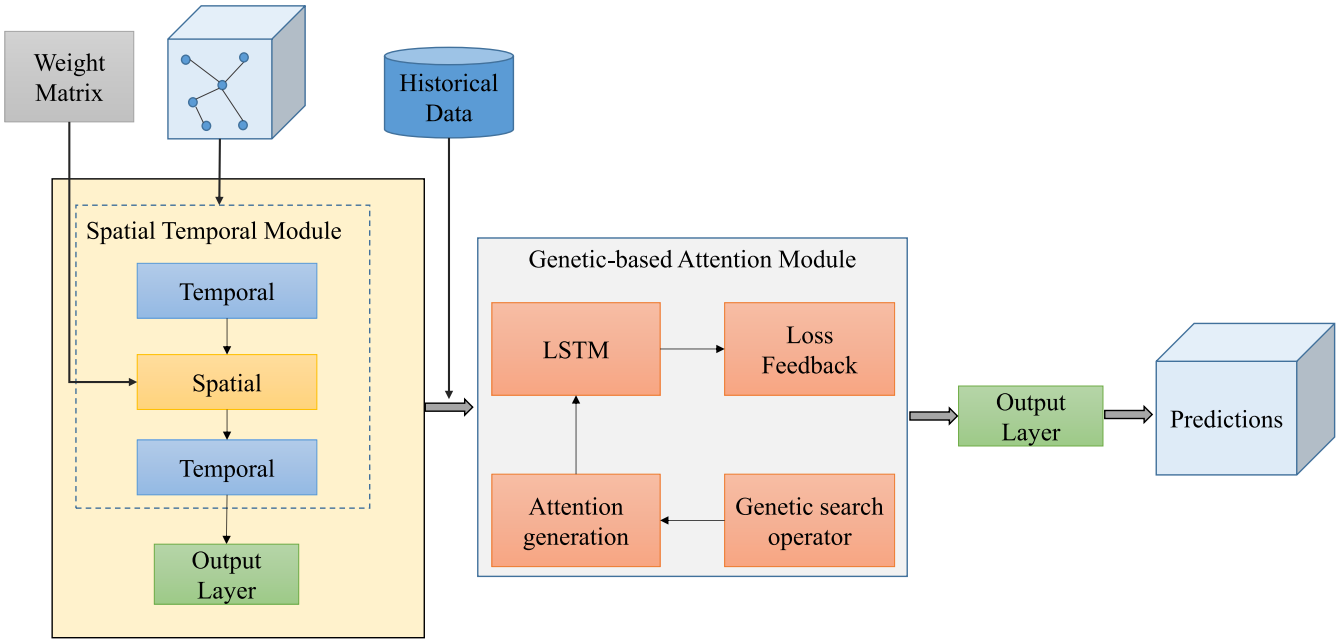

FIGURE 3. PV short-term forecasting framework.

by genetic-based search operator, then feeds the input matrix into LSTM layer to get the loss for further iterations and to obtain better weights. Subsequently, the model will be trained until loss convergence and obtains the predicted power result. The flow of model training is shown in Fig 4.

1) The historical meteorological data are normalized and mapped to the interval [0, 1];
2) Weather factors such as solar irradiance are sent to the spatial temporal module to predict the missing values;
3) The completed meteorological data is sent to genetic-based attention module as input to predict the actual power generation of distributed photovoltaic power station;
4) Calculate the loss function and judge whether the training has converged;
5) If loss has converged turn to the end, otherwise jump to step 2 to start a new round of training.

B. SPATIAL-TEMPORAL MODULE

In this work, we define the distribution of PV plants with structured meteorological time series in undirected graph, $G_t = (V_t, \varepsilon, W)$, where V_t is a finite of vertices each of which means the meteorological factor at time t, ε is the set of edges and W is the adjacency matrix of the graph. The meteorological factor data prediction on graphs can be represented by

$$[d_{t-P+1}, \ldots, d_t] \xrightarrow{f} \left[\hat{d}_{t+1}, \ldots \hat{d}_{t+H}\right] \tag{2}$$

where P is the number of historical data, H is the number of the predicted data.

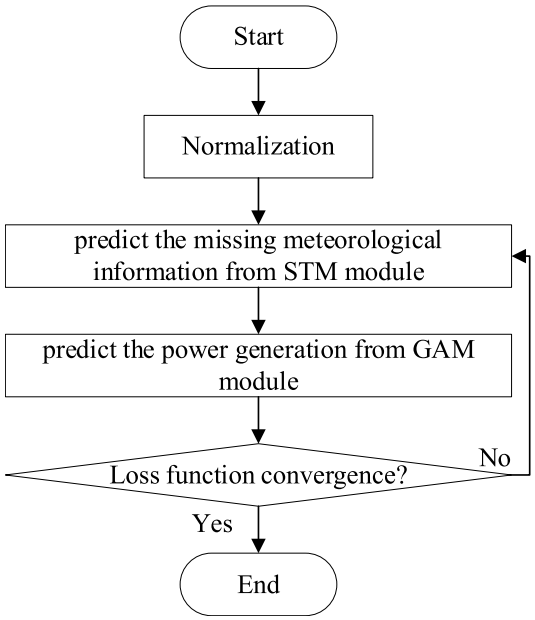

FIGURE 4. Flow chart of model training.

1) SPATIAL SUB-MODULE

Graph Convolutional Networks (GCN)[28] generalizes CNN to graph domains by computing in the spectral domain with the graph Fourier transform as

$$g_\theta(.) * x = \mathrm{U} g_\theta(\Lambda) U^T x \tag{3}$$

where U is the matrix of eigenvectors of the normalized graph Laplacian $\mathrm{L} = I_N - D^{-1/2} A D^{-1/2} = U \Lambda U$, with a diagonal

matrix of its eigenvalues Λ and $U^T x$ being the graph Fourier transform of x.

Organizing the data as a graph according to the distribution of PV plants can make efficient use of spatial information, meanwhile we apply the graph convolution operation directly on the structured data to extract deep patterns and features in the space domain. However, the matrix multiplication of eigenvectors in (3) might be computationally expensive for large graphs, Chebyshev polynomials approximation and layer-wise linear formulation can be applied to overcome it.

To reduce the time complexity, the filter is approximated by a truncated expansion in terms of Chebyshev polynomials $T_k(x)$ up to K^{th} order. Then we can rewrite graph convolution as

$$g_\theta(\cdot) * x \approx \sum_{k=0}^{K} \theta_k T_k(\check{L}) x \tag{4}$$

where $\check{L} = 2\mathrm{L}/\lambda_{max} - I_n$ can be computed by $\left(U \Lambda U^T\right)^k = U \Lambda^k U^T$. The time complexity of (4) is reduced by computing the K-local convolution through polynomial approximation.

By limiting $\mathrm{K} = 1$, the graph convolution function can be made linear on the graph Laplacian. Further, since the neural network can adapt to scale variation, we can approximate $\lambda_{max} = 2$.

$$g_\theta(\cdot) * x \approx \theta_0 x - \theta_1 (D^{-\frac{1}{2}} W D^{-\frac{1}{2}}) x \tag{5}$$

where θ_0 and θ_1 are two shared filter parameters. To reduce the occurrence of overfitting and numerical manipulation, the θ_0 and θ_1 can be exchanged to a single parameter θ by letting $\theta = \theta_0 = -\theta_1$; $\tilde{W} = W + I_N$ and $\tilde{D}_{ii} = \sum_j \tilde{W}_{ij}$.Then we have the following expression as:

$$g_\theta(\cdot) * x = \theta \left(\tilde{D}^{-\frac{1}{2}} W \tilde{D}^{-\frac{1}{2}}\right) x \tag{6}$$

2) TEMPOROL SUB-MODULE

RNN-liked models have been suffered from time-consuming issue and the inability to cope with variable data due to the complicated gate mechanism, while CNNs have the advantage of fast training and can achieve parallel training process by stacking convolutional layers. Therefore, we apply gated linear unit with a K_t width kernel and 1-D dilated convolution on the time dimension of the input data, as shown in Fig. 5.

The input of temporal sub-module can be viewed as a sequence $\mathrm{Z} \in \mathbb{R}^{M \times C_I}$ of length M with C_i channels and the kernel size is $\Gamma \in \mathbb{R}^{K_t \times C_I \times 2C_o}$. After entering the module, two separate dilated convolution operations are performed to obtain two output of the same size as $[AB] \in \mathbb{R}^{(M-K_t+1) \times C_o}$.

The d-dilated convolution operation can be represented as

$$\mathrm{F}(\mathrm{x}) = \sum_{i=0}^{k-1} f(i) \cdot x_{t-d \times i} \tag{7}$$

where d is the dilated parameter which controls the skipping distance, $f \in \mathbb{R}^k$ is the kernel, x_t is the t-th value of the sequence x.

The A and B pass through the sigmoid function and fusion operation respectively, and finally Hadamard product is performed to acquire the result. The sigmoid function helps to filter the inputs that are instrumental in discovering the dynamic change pattern of the data, and the nonlinear gate can capture the information of the data in general. Finally, the temporal convolution can be defined as

$$h(\Gamma)\,\mathrm{Z} = \mathrm{F}(A) \otimes \mathrm{F}(\sigma(B)) \tag{8}$$

where σ is the sigmoid function; $\otimes$ is the element-wise Hadamard product operation.

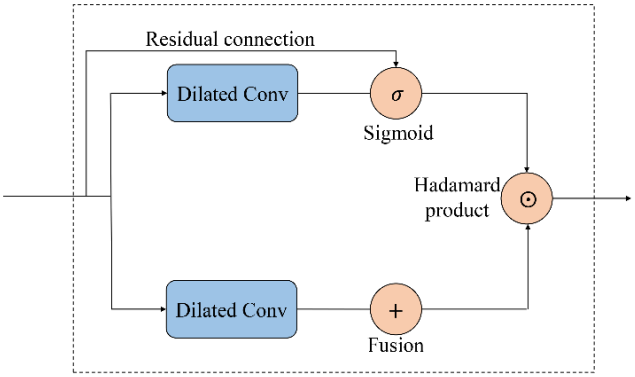

FIGURE 5. The structure of temporal sub-module.

C. GENETIC-BASED ATTENTION MODULE

The genetic-based attention module (GAM) consists of the LSTM model, attention mechanism and genetic-based search operator (GSO). The input of GAM is the predicted result concentrate on historical meteorological data and historical power data. The LSTM is used to deal with long-term dependencies, the attention mechanism enhances the influence of important factors, and the GSO searches for optimal weights. As a specific of the recurrent neural network, LSTM [29] was proposed, which introduced the memory cell and gate mechanism to perform time-series data efficiently. To begin with, the attention weights for N length of time steps are expressed as:

$$\mathrm{W}_{att} = (W_1, W_2, \ldots, W_N) \tag{9}$$

Then the importance-based input data (PV output power and meteorological factor data) with attention weights are defined as:

$$\tilde{X}_t = (x_{1t} W_1, x_{2t} W_2, \ldots, x_{Nt} W_N) \tag{10}$$

At time t, sequence input vector $\tilde{X}_t$, hidden layer output h_{t-1} and cell state C_{t-1} are fed into cell, then get LSTM hidden layer output h_t and cell state C_t as output. The calculation of cell state C_t is combines the state of previous period and state of current candidate cell whose proportions are occupied by the forget gate and input gate respectively. The candidate cell state $\tilde{C}_t$ is calculated by a hyperbolic tangent activation function. The update progress of LSTM can be described as follows:

$$f_t = \sigma(W_f \cdot \left[h_{t-1}, \tilde{X}_t\right] + b_f) \tag{11}$$

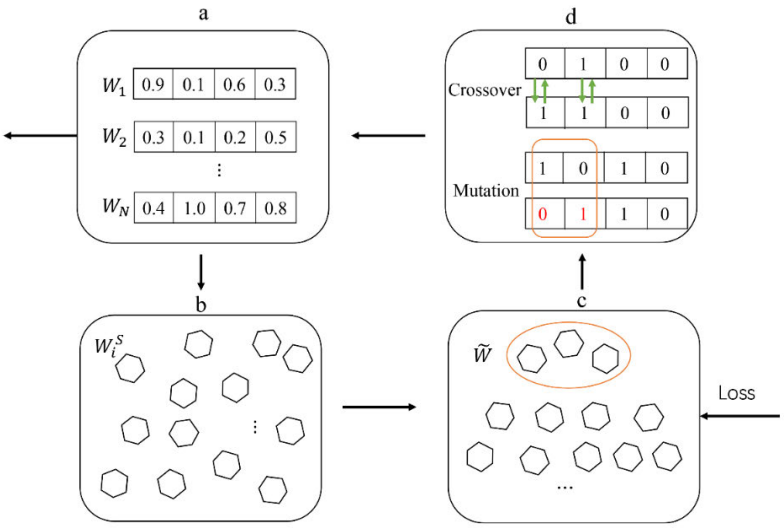

FIGURE 6. Basic steps of GSO.

$$i_t = \sigma\left(W_i \cdot \left[h_{t-1}, \tilde{X}_t\right] + b_i\right) \tag{12}$$

$$o_t = \sigma(W_o \cdot \left[h_{t-1}, \tilde{X}_t\right] + b_o) \tag{13}$$

$$\tilde{C}_t = tanh(W_h \cdot \left[h_{t-1}, \tilde{X}_t\right] + b_c) \tag{14}$$

$$C_t = f_t \cdot C_{t-1} + i_t \cdot \tilde{C}_t \tag{15}$$

$$h_t = o_t \cdot \tanh(C_t) \tag{16}$$

where W_f, W_i, W_o, W_c denote weight parameters and b_f, b_i, b_i, b_c denote bias parameters of forget gate, bias of input gate, bias of output gate and bias of internal cell state, respectively; and σ stands for the sigmoid activation function.

The attention mechanism [30] helps assign more weight to the critical inputs while giving less weight to the rest of the analysis to soften their influence. We use a genetic-based search operator (GSO) to train attention weights by taking training loss as a reference to acquire optimal parameters in the attention layer of the LSTM network for better utilizing the intrinsic relationship between meteorological factors and power generation data. The basic steps of GSO are shown in Fig. 6. The detailed process of GSO will be introduced as follows.

The attention weights set $\mathrm{W}_{att} = (W_1, W_2, \ldots, W_M)$ is encoded by binary values as $W^S = \left(W_1^S, W_2^S, \ldots, W_M^S\right)$ and the initial code is randomly generated. The W_i which denotes attention weights for historical generated data and meteorological factors will be delivered to the networks and produce corresponding fitness score based on the training loss. Then the fittest subset space $\widetilde{W_{att}}$ is selected according to the fitness score of corresponding $W^S = \left(W_1^S, W_2^S, \ldots, W_M^S\right)$ where the selected subsets will be equally divided into N segments[22] such as $W_k^S = \left(S_k^1, S_k^2, \ldots, S_k^N\right)$. New attention weights space will be rebuilt by crossover and mutation operation.

- Crossover: Suppose the selected subsets are W_i^S and W_j^S, the segments of both subsets will be chosen randomly for exchanging from themselves until the cross number is reached and the cross number is fixed. For example, S_j^N and S_i^N will generate S_k^N after crossover.
- Mutation: In the new offspring formed, some of their segments may be mutated with random probability, which means that certain positions in the string can be flipped. In this work, the odd or even index segments which decided by random judgment will be flipped in the new generated string.

We will traverse the subspace $\widetilde{W_{att}}$ repeatedly until its size reach the default value M when rebuilding the optimization space. The GSO is shown in the optimization problem as follows:

$$\min L(y_p\left(F_{att}\left(\theta, \mathrm{W}_{att}\right)\right), y) \tag{17}$$

where $L(\cdot)$ is loss function, $F_{att}(\cdot)$ is the entire network, θ is parameter space in LSTM when acquiring predicted values, y_p denotes predicted output, y denotes actual value.

IV. EVALUATION

A. METRICS

In this paper, three metrics are used to evaluate the forecasting accuracy of our model, which are the mean absolute error (MAE), the mean absolute percentage error (MAPE) and the root mean square error (RMSE). The definitions of these three evaluation indexes are shown as (18), (19) and (20):

$$\delta_{MAE} = \frac{1}{n}\sum_{i=1}^{n}\left|y_i - \hat{y}_i\right| \tag{18}$$

$$\delta_{MAPE} = \frac{1}{n}\sum_{i=1}^{n}\frac{\left|y_i - \hat{y}_i\right|}{y_i} \tag{19}$$

$$\delta_{RMSE} = \sqrt{\frac{1}{n}\sum_{i=1}^{n}\left(y_i - \hat{y}_i\right)^2} \tag{20}$$

where y_i is the actual value, $\hat{y}_i$ is the predicted value of the model and n is the number of testing samples.

B. BENCHMARK ALGORITHMS

To verify the performance of the proposed model for day ahead PV power generation forecasting, we set contrast experiments with some benchmark models. The GRU [31] and CNN [32] were selected as the benchmark for the solar irradiance prediction experiment. The CNN [33], LSTM [5], GT-DBN [34], W-RVFL [36] and WPD-LSTM [35] models were selected as competitors for power generation prediction experiment. The actual PV power generation data and meteorological data of three PV stations were applied in the experiments.

V. RESULT AND DISCUSSION

In this section, we conduct a series of comparative experiments to verify the performance of our proposed model. First, the STM is utilized to predict solar irradiance for the five days ahead in the training set to cope with missing data. The adjacency matrix fed into STM stores the distances between PV plants, which is calculated from their latitude and longitude. The predicted data is then concentrated with the original historical meteorological data and fed into GAM together with the historical generation data for the final generation forecast for the next 24 hour. These two predictions for the next 24 hour will be compared with different benchmark experiments.

A. PERFORMANCE OF SPATIAL-TEMPORAL MODULE

The spatial-temporal module uses spatio-temporal features to predict the five days ahead solar irradiance in the missing regions. The prediction results are shown in Table 4. Since solar irradiance can only be collected during the day, the predictions for the next 5 days from 8:00-18:00 are shown in Fig. 7. No-Spa is the module that removes the spatial sub-module. The results of No-Spa are much more accurate than GRU and CNN, which indicates that the temporal sub-module can extract more global temporal information. The STM is superior to No-Spa, proving that capturing spatial and temporal features is essential and effective for solar irradiance prediction. The predicted result will be fed into GAM as part of the input for generation power forecasting.

TABLE 4. Summary of solar irradiance prediction.

model	MAE	RMSE	MAPE
GRU	128.448	147.567	18.691
CNN	119.082	136.853	17.838
No-Spa	110.216	130.803	15.972
STM	**106.542**	**123.673**	**15.951**

B. POWER GENERATION PREDICTION FOR A DAY AHEAD

1) OVERALL RESULT

The categorized meteorological data show that rainy weather data accounts for only 16.7% of the overall data, while sunny weather data is only 8.3%.

For the overall evaluation, the results of the three power plants are taken together to calculate the metrics. The solar irradiance obtained from STM predictions provides the basis for the forecasting of photovoltaic power generation. The overall predicted results were shown in Table 5. The prediction accuracy of our STGANet model is higher than all benchmark methods, and it has the best performance overall compared to methods in general under different weather conditions. The MAPE of W-RVFL under rainy conditions is lower than STGANet because the PV plant generation is close to 0 in the evening on a rainy day. Due to the way MAPE is calculated, even minor errors can cause significant fluctuations in percentage. Compared to the other comparable models, the average MAE metrics of STGANet under cloudy conditions decreased by 2.993, 2.848, 2.659, 2.663 and 0.996, respectively. Similarly, the average MAE metrics under rainy conditions were reduced by 7.086, 2.148, 3.048, 1.133 and 1.052, respectively.

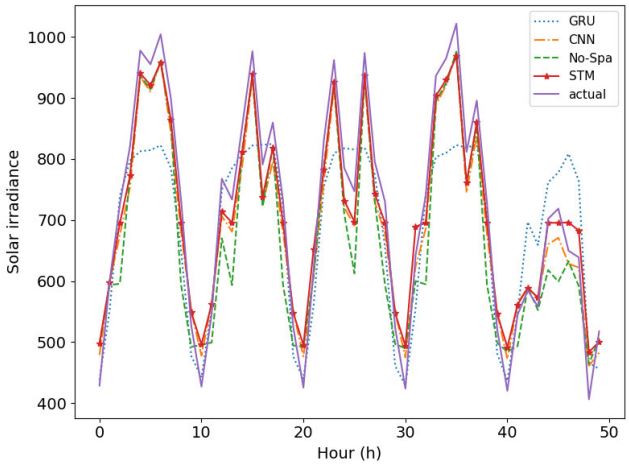

FIGURE 7. Solar irradiance prediction result (only contains 8:00-18:00).

In STGANet, the errors calculated on cloudy days are mostly smaller than those on sunny and rainy days because the sample size on cloudy days is more significant than that on sunny and rainy days. Therefore the model can learn the features better. However, despite the small sample size of rainy and sunny days, STGANet still obtains promising results, indicating its vital learning and generalization ability.

2) ANLYZE OF RESULTS IN DIFFERENT WEATHER CONDITION

The summaries of the forecasting performance of the sunny day, cloudy day and rainy day are shown in Table 6, Table 7 and Table 8, respectively. During sunny days, the power generation and solar irradiance will vary regularly together. While in cloudy and rainy days, the solar irradiance and output power fluctuate more and have smaller values, with more volatility and less regularity. Because the sample size of sunny days is too small, its MAE and RMSE are larger than other weather conditions. Because the fluctuation of solar irradiance on rainy days is too large, its MAPE is much larger than that of sunny and cloudy days. Most methods

TABLE 5. Summary of the overall performance for a day ahead.

Metrics	Methods	Sunny Days	Cloudy Days	Rainy Days
MAE	CNN	3.535	4.622	8.362
	LSTM	4.842	4.477	3.424
	GT-DBN	4.252	4.288	4.324
	W-RVFL	5.404	4.292	2.409
	WPD-LSTM	2.722	2.625	2.328
	STGANet	**2.002**	**1.629**	**1.276**
RMSE	CNN	20.884	34.860	88.369
	LSTM	25.092	21.715	14.219
	GT-DBN	21.563	23.251	22.801
	W-RVFL	11.980	29.000	40.975
	WPD-LSTM	5.234	4.008	6.812
	STGANet	**5.085**	**3.598**	**2.233**
MAPE(%)	CNN	25.648	41.903	354.639
	LSTM	23.353	27.528	75.719
	GT-DBN	20.679	26.125	109.807
	W-RVFL	18.457	18.517	**34.585**
	WPD-LSTM	10.570	12.081	89.587
	STGANet	**9.399**	**9.902**	76.301

TABLE 6. Summary of the performance of the cloudy day for a day ahead.

Metrics	Methods	Plant-1	Plant-2	Plant-3
MAE	CNN	3.081	6.736	4.066
	LSTM	5.713	4.484	3.246
	GT-DBN	6.027	5.031	1.937
	W-RVFL	3.990	2.673	6.187
	WPD-LSTM	2.446	1.921	1.510
	STGANet	**2.365**	**1.606**	**0.921**
RMSE	CNN	16.305	55.985	32.435
	LSTM	33.051	20.775	11.403
	GT-DBN	6.027	27.185	4.0496
	W-RVFL	23.261	13.574	49.895
	WPD-LSTM	6.128	3.698	3.198
	STGANet	**6.103**	**3.196**	**1.510**
MAPE(%)	CNN	13.256	66.623	38.980
	LSTM	28.521	35.882	18.310
	GT-DBN	28.370	38.573	11.629
	W-RVFL	13.881	14.210	27.178
	WPD-LSTM	13.221	18.166	8.918
	STGANet	**12.493**	**12.994**	**4.287**

perform better in plant-1 and plant-3 than plant-2, perhaps caused by differences in geographic location and hardware devices.

As shown in Table 6, all metrics of STGANet performed well in the cloudy experiment, with minimal prediction errors and stable results, indicating its validity and accuracy.

As shown in Table 7, the regularity of meteorological factors data and PV power generation data decreases in rainy conditions compared to cloudy days. While RMSE and MAE of STGANet and other benchmark models have decreased, their MAPE has increased. Compared with the CNN, LSTM, GT-DBN, W-RVFL and WPD-LSTM methods, the MAPE

TABLE 7. Summary of the performance of the rainy day for a day ahead.

Metrics	Methods	Plant-1	Plant-2	Plant-3
MAE	CNN	7.500	8.000	9.339
	LSTM	4.028	3.915	2.123
	GT-DBN	5.827	4.966	1.904
	W-RVFL	1.506	2.621	3.296
	WPD-LSTM	2.473	2.184	2.121
	STGANet	**1.425**	**1.470**	**0.932**
RMSE	CNN	62.845	78.582	117.327
	LSTM	18.725	16.986	5.679
	GT-DBN	36.383	27.325	3.827
	W-RVFL	2.378	15.648	17.071
	WPD-LSTM	7.633	5.983	4.896
	STGANet	**2.377**	**3.231**	**1.057**
MAPE(%)	CNN	164.670	446.788	416.529
	LSTM	58.742	109.420	34.785
	GT-DBN	110.549	139.085	56.709
	W-RVFL	58.787	**29.225**	42.535
	WPD-LSTM	59.888	108.701	75.906
	STGANet	**52.084**	153.574	**18.680**

TABLE 8. Summary of the performance of the sunny day for a day ahead.

Metrics	Methods	Plant-1	Plant-2	Plant-3
MAE	CNN	2.859	4.834	3.682
	LSTM	6.022	4.810	3.652
	GT-DBN	5.788	4.679	2.124
	W-RVFL	4.925	3.751	7.941
	WPD-LSTM	2.816	2.810	2.139
	STGANet	**2.717**	**2.029**	**1.224**
RMSE	CNN	8.655	34.514	18.915
	LSTM	36.768	24.392	13.784
	GT-DBN	35.806	22.994	4.953
	W-RVFL	31.226	3.751	75.058
	WPD-LSTM	8.401	5.361	5.989
	STGANet	**7.893**	**5.301**	**1.892**
MAPE(%)	CNN	11.554	42.280	20.150
	LSTM	23.891	29.745	14.916
	GT-DBN	21.365	30.107	8.342
	W-RVFL	15.166	21.568	25.220
	WPD-LSTM	16.792	15.268	8.7150
	STGANet	**11.454**	**11.842**	**4.245**

metric of plant-1 has been decreased by 112.586%, 6.658%, 58.465%, 6.703% and 7.804%, respectively.

Under sunny conditions, as shown in Table 8, due to the regular fluctuation of solar irradiance, the predictions of the models vary less among all benchmark models. However, our STGANet still achieves the best results. Moreover, the result proves that our model has a strong learning ability even for small sample data.

The results of the proposed model for PV plant-1 under different weather conditions (i.e., sunny day, cloudy day, rainy day) are shown in Fig. 8. The curve for sunny days shows a clear trend of increasing and decreasing, with the peak of

TABLE 9. Summary of the performance for the next five days.

	CNN	LSTM	GT-DBN	W-RVFL	WPD-LSTM	STGANet
MAE	9.224	5.264	6.253	6.611	3.088	**2.956**
RMSE	30.359	15.033	17.053	10.314	7.664	**5.531**
MAPE(%)	36.678	64.786	29.463	19.382	17.269	**14.843**

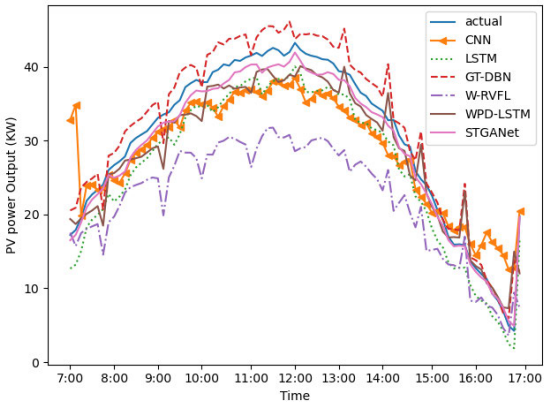

(a) PV output power of plant-1 in sunny condition.

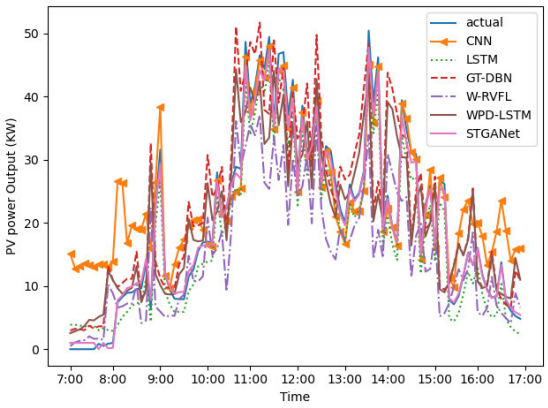

(b) PV output power of plant-1 in cloudy condition.

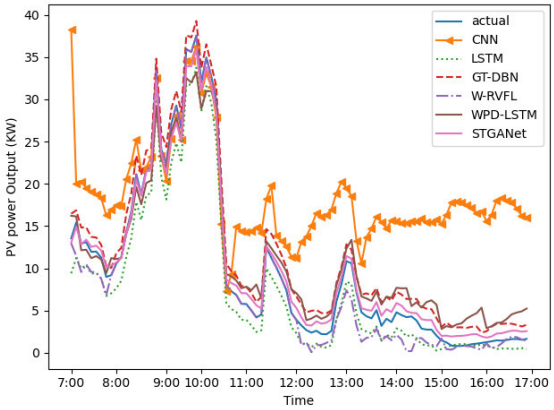

(c) PV output power of plant-1 in rainy condition.

FIGURE 8. PV output power of plant-1.

power generation occurring at noon. The curve for cloudy days, on the other hand, shows significant fluctuations, and no significant peak appears. The curve for rainy days is more volatile than other weathers, and the power generation value decreases significantly in the afternoon, and even to 0 in the last two hours. The predicted curve of CNN fluctuates fiercely when the actual curve fluctuates, resulting in significant discrepancies in the output. The LSTM and RNN outperform CNN. Particularly, the predicted curve of our STGANet model fits better than any other methods. The prediction curves of our model almost matched the actual measured curve of PV power generation in all weather conditions, and the prediction curve and actual curve matched a little less well under rainy conditions.

C. POWER GENERATION PREDICTION FOR THE NEXT FIVE DAYS

In order to investigate the performance of the STGANet model in different time horizons, we also conducted long-term experiments to verify the model's predictive performance for the next five days of generation. Table 9 lists the overall performance of the compared models. As shown in the table, the prediction error of each model is increased compared to the result of sunny days in the short-term prediction. However, all of them are lower than rainy days, perhaps because there are fewer rainy days and more sunny days in these five days. There is considerable improvement in error measures and error variance of STGANet compared to all the other forecast models. The results at each prediction horizon generated by the CNN method are the worst compared to other benchmarks. At all prediction horizons in the case studies, the proposed method has the smallest RMSE metrics, which shows the best forecasting performance compared to other methods.

VI. CONCLUSION

In this paper, a novel deep learning network called STGANet is proposed, which focuses on short-term distributed PV power prediction. This model integrates the spatial-temporal graph convolution for solar irradiance prediction and a genetic-based attention mechanism for power prediction. Specifically, we utilize the spatial connection between PV plants by graph convolution for prediction and capture both the global and global dependencies by attention mechanism. This method can overcome the missing of weather data in distributed photovoltaic power stations, so as to achieve accurate power generation prediction. A real-world dataset collected from PV power plants in southeastern China is employed for experiments. We conducted a comprehensive comparative study to compare the proposed STGANet method with existing state-of-the-art methods, including CNN, LSTM,

GT-DBN, W-RVFL, and WPD-LSTM models over two different error ranges of one day lead and five days lead. All prediction ranges were compared using three different error metrics, i.e., MAE, RMSE, and MAPE. Compared to the CNN, LSTM, GT-DBN, W-RVFL, and WPD-LSTM models, the average MAE metrics of STGANet under cloudy conditions decreased by 2.993, 2.848, 2.659, 2.663 and 0.996, respectively. The results show that our method has more competitive effects than other models in PV power forecasting, which proves our method could effectively approximate optimal attention weights and efficient mining of spatial-temporal dependencies.

REFERENCES

[1] S. Massucco, G. Mosaico, M. Saviozzi, and F. Silvestro, "A hybrid technique for day-ahead PV generation forecasting using clear-sky models or ensemble of artificial neural networks according to a decision tree approach," *Energies*, vol. 12, no. 7, p. 1298, Apr. 2019.

[2] M. Liu, L. Tan, and S. Cao, "Theoretical model of energy performance prediction and BEP determination for centrifugal pump as turbine," *Energy*, vol. 172, pp. 712–732, Apr. 2019.

[3] Y. Liu and L. Tan, "Theoretical prediction model of tip leakage vortex in a mixed flow pump with tip clearance," *J. Fluids Eng., Trans. ASME*, vol. 142, no. 2, pp. 21203–21214, Feb. 2020.

[4] A. T. Eseye, M. Lehtonen, T. Tukia, S. Uimonen, and R. J. Millar, "Adaptive predictor subset selection strategy for enhanced forecasting of distributed PV power generation," *IEEE Access*, vol. 7, pp. 90652–90665, 2019.

[5] M. Chai, F. Xia, S. Hao, D. Peng, C. Cui, and W. Liu, "PV power prediction based on LSTM with adaptive hyperparameter adjustment," *IEEE Access*, vol. 7, pp. 115473–115486, Aug. 2019.

[6] M. N. Akhter, S. Mekhilef, H. Mokhlis, and N. M. Shah, "Review on forecasting of photovoltaic power generation based on machine learning and metaheuristic techniques," *IET Renew. Power Gener.*, vol. 13, no. 7, pp. 1009–1023, May 2019.

[7] U. K. Das, K. S. Tey, M. Seyedmahmoudian, S. Mekhilef, M. Y. I. Idris, W. Van Deventer, B. Horan, and A. Stojcevski, "Forecasting of photovoltaic power generation and model optimization: A review," *Renew. Sustain. Energy Rev.*, vol. 81, pp. 912–928, Jan. 2018.

[8] Y. Li, Y. Su, and L. Shu, "An ARMAX model for forecasting the power output of a grid connected photovoltaic system," *Renew. Energy*, vol. 66, pp. 78–89, Jun. 2014.

[9] J. Yang, Z. Hou, and M. Zhan, "Simulation of pedestrian dynamic using a vector floor field model," *Int. J. Mod. Phys. C*, vol. 24, no. 4, Apr. 2013, Art. no. 1350023.

[10] Y. K. Semero, J. Zhang, and D. Zheng, "PV power forecasting using an integrated GA-PSO-ANFIS approach and Gaussian process regression based feature selection strategy," *CSEE J. Power Energy Syst.*, vol. 4, no. 2, pp. 210–218, Jun. 2018.

[11] C. Persson, P. Bacher, T. Shiga, and H. Madsen, "Multi-site solar power forecasting using gradient boosted regression trees," *Sol. Energy*, vol. 150, pp. 423–436, Jul. 2017.

[12] J. Wang, B. Leng, J. Wu, H. Du, and Z. Xiong, "MetroEye: A weather-aware system for real-time metro passenger flow prediction," *IEEE Access*, vol. 8, pp. 129813–129829, 2020.

[13] J. Wang, Z. Qian, J. Wang, and Y. Pei, "Hour-ahead photovoltaic power forecasting using an analog plus neural network ensemble method," *Energies*, vol. 13, no. 12, p. 3259, Jun. 2020.

[14] G. Cervone, L. Clemente-Harding, S. Alessandrini, and L. D. Monache, "Short-term photovoltaic power forecasting using artificial neural networks and an analog ensemble," *Renew. Energy*, vol. 108, pp. 274–286, Aug. 2017.

[15] F. Grimaccia, S. Leva, M. Mussetta, and E. Ogliari, "ANN sizing procedure for the day-ahead output power forecast of a PV plant," *Appl. Sci.*, vol. 7, no. 6, p. 622, Jun. 2017.

[16] J. Wang, R. Ran, Z. Song, and J. Sun, "Short-term photovoltaic power generation forecasting based on environmental factors and GA-SVM," *J. Electr. Eng. Technol.*, vol. 12, no. 1, pp. 64–71, Jan. 2017.

[17] M. Malvoni, M. G. De Giorgi, and P. M. Congedo, "Data on support vector machines (SVM) model to forecast photovoltaic power," *Data Brief*, vol. 9, pp. 13–16, Dec. 2016.

[18] H. S. Jang, K. Y. Bae, H.-S. Park, and D. K. Sung, "Solar power prediction based on satellite images and support vector machine," *IEEE Trans. Sustain. Energy*, vol. 7, no. 3, pp. 1255–1263, Jul. 2016.

[19] G. M. de Paiva, S. P. Pimentel, B. P. Alvarenga, E. G. Marra, M. Mussetta, and S. Leva, "Multiple site intraday solar irradiance forecasting by machine learning algorithms: MGGP and MLP neural networks," *Energies*, vol. 13, no. 11, p. 3005, Jun. 2020.

[20] Y. Sun, B. Leng, and W. Guan, "A novel wavelet-SVM short-time passenger flow prediction in Beijing subway system," *Neurocomputing*, vol. 166, pp. 109–121, Oct. 2015.

[21] C. Huang, L. Cao, N. Peng, S. Li, J. Zhang, L. Wang, X. Luo, and J.-H. Wang, "Day-ahead forecasting of hourly photovoltaic power based on robust multilayer perception," *Sustainability*, vol. 10, no. 12, p. 4863, Dec. 2018.

[22] S. Wang, Y. Sun, Y. Zhou, R. J. Mahfoud, and D. Hou, "A new hybrid short-term interval forecasting of PV output power based on EEMD-SE-RVM," *Energies*, vol. 13, no. 1, p. 87, Dec. 2019.

[23] M. Q. Raza, N. Mithulananthan, and A. Summerfield, "Solar output power forecast using an ensemble framework with neural predictors and Bayesian adaptive combination," *Sol. Energy*, vol. 166, pp. 226–241, May 2018.

[24] P. Lin, Z. Peng, Y. Lai, S. Cheng, Z. Chen, and L. Wu, "Short-term power prediction for photovoltaic power plants using a hybrid improved *K* means-GRA-Elman model based on multivariate meteorological factors and historical power datasets," *Energy Convers. Manage.*, vol. 177, pp. 704–717, Dec. 2018.

[25] F. Harrou, F. Kadri, and Y. Sun, "Forecasting of photovoltaic solar power production using LSTM approach," in *Advanced Statistical Modeling, Forecasting, and Fault Detection in Renewable Energy Systems*. London, U.K.: IntechOpen, 2020.

[26] Y. Li, Z. Zhu, D. Kong, H. Han, and Y. Zhao, "EA-LSTM: Evolutionary attention-based LSTM for time series prediction," *Knowl.-Based Syst.*, vol. 181, Oct. 2019, Art. no. 104785.

[27] H. Zhou, Y. Zhang, L. Yang, Q. Liu, K. Yan, and Y. Du, "Short-term photovoltaic power forecasting based on long short term memory neural network and attention mechanism," *IEEE Access*, vol. 7, pp. 78063–78074, 2019.

[28] B. Yu, H. Yin, and Z. Zhu, "Spatio-temporal graph convolutional networks: A deep learning framework for traffic forecasting," in *Proc. 27th Int. Joint Conf. Artif. Intell.*, Stockholm, Sweden, Jul. 2018, pp. 3634–3640.

[29] S. Hochreiter and J. Schmidhuber, "Long short-term memory," *Neural Comput.*, vol. 9, no. 8, pp. 1735–1780, Nov. 1997.

[30] T. Luong, H. Pham, and C. D. Manning, "Effective approaches to attention-based neural machine translation," in *Proc. EMNLP*, 2015, pp. 1412–1421.

[31] J. Wojtkiewicz, M. Hosseini, R. Gottumukkala, and T. L. Chambers, "Hour-ahead solar irradiance forecasting using multivariate gated recurrent units," *Energies*, vol. 12, no. 21, p. 4055, Oct. 2019.

[32] N. Dong, J.-F. Chang, A.-G. Wu, and Z.-K. Gao, "A novel convolutional neural network framework based solar irradiance prediction method," *Int. J. Electr. Power Energy Syst.*, vol. 114, Jan. 2020, Art. no. 105411.

[33] N. Park and H. K. Ahn, "Multi-layer RNN-based short-term photovoltaic power forecasting using IoT dataset," in *Proc. AEIT Int. Annu. Conf. (AEIT)*, Florence, Italy, Sep. 2019, pp. 1–5.

[34] G. W. Chang and H.-J. Lu, "Integrating gray data preprocessor and deep belief network for day-ahead PV power output forecast," *IEEE Trans. Sustain. Energy*, vol. 11, no. 1, pp. 185–194, Jan. 2020.

[35] P. Li, K. Zhou, X. Lu, and S. Yang, "A hybrid deep learning model for short-term PV power forecasting," *Appl. Energy*, vol. 259, Feb. 2020, Art. no. 114216.

[36] V. Kushwaha and N. M. Pindoriya, "A SARIMA-RVFL hybrid model assisted by wavelet decomposition for very short-term solar PV power generation forecast," *Renew. Energy*, vol. 140, pp. 124–139, Sep. 2019.

[37] D. Korkmaz, H. Acikgoz, and C. Yildiz, "A novel short-term photovoltaic power forecasting approach based on deep convolutional neural network," *Int. J. Green Energy*, vol. 18, no. 5, pp. 525–539, Feb. 2021.

[38] C. Yildiz and H. Acikgoz, "A kernel extreme learning machine-based neural network to forecast very short-term power output of an on-grid photovoltaic power plant," *Energy Sources A, Recovery, Utilization, Environ. Effects*, vol. 43, no. 4, pp. 395–412, Aug. 2020.

TAO FAN received the M.S. degree from Shandong University. He is currently a Professorate Senior Engineer with State Grid Corporation of China, where he is also the Vice Director of the Internet Department. He is the Secretary General of central enterprise e-commerce alliance. His research interests include enterprise informatization, power system automation, and energy internet. He has won the First Prize of China Electric Power Science and Technology Award and the First Prize of Science and Technology Progress of State Grid Corporation of China.

TAO SUN received the B.S. degree from the Electrical Engineering Department, Shanghai Jiaotong University, in 1990. He is currently the Vice General Manager of State Grid E-Commerce Company Ltd. His research interests include power system automation, energy internet, new energy, and distributed photovoltaic power station operation monitoring. He received the Senior Engineer Qualification Certificate, in 2001.

HU LIU received the B.S. degree in mechanical engineering and automation, computer science and technology and the M.S. degree in mechanical and electrical engineering from North China Electric Power University, in 2003 and 2006, respectively. He is currently the Deputy Director of the Internet Department, State Grid Corporation of China. His research interests include power marketing, power grid production, and energy services. He won the First Prize of Geographic Information Technology Progress of China Geographic Information Industry Association, the Special Award of Scientific Progress of State Grid Corporation of China, and the First Prize of China Electric Power Innovation.

XIANGYING XIE received the B.S. degree in computer science and technology from Wuhan University of Science and Technology, in 2003, and the M.S. degree in software engineering from Sichuan University. He is currently pursuing the Ph.D. degree with Beihang University. He is a Deputy General Manager of photovoltaic cloud (e-commerce poverty alleviation) with the Business Department, State Grid E-Commerce Company Ltd., and a General Manager of State Grid New Energy Cloud Technology Company Ltd. His research interest includes the new energy industry internet. He won the honor of "Outstanding Individual" in SASAC Central Enterprise Innovation Achievement Exhibition.

ZHIXIONG NA received the B.S. degree in thermal engineering from Changzhou University, in 1996, the M.S. degree in computer application from the University of Science and Technology of China, in 2001, and the M.B.A. degree from the University of International Business and Economics, in 2009. He is currently a Professor with State Grid E-Commerce Company Ltd. His research interests include industrial automation and new energy industrial internet.